Investigation of Poly(ethersulfone)/Polyvinylpyrrolidone ultrafiltration membrane degradation by contact with sodium hypochlorite through FTIR mapping and two-dimensional correlation spectroscopy

J. Chokki, G. Darracq, P. Poelt, J. Baron, H. Gallard, M. Joyeux, B. Teychené

Investigation of Poly(ethersulfone)/Polyvinylpyrrolidone ultrafiltration membrane degradation by contact with sodium hypochlorite through FTIR mapping and two-dimensional correlation spectroscopy.

J. Chokki[1,2], G. Darracq[2], P. Poelt[3], J. Baron[2], H. Gallard[1], M. Joyeux[2], B. Teychené[1]*

[1] *Institut de Chimie des Milieux et Matériaux de Poitiers (IC2MP – UMR CNRS 7285), Université de Poitiers, École Nationale Supérieure d'Ingénieurs de Poitiers, 7 rue Marcel Doré, Bâtiment 16, TSA 41105, 86073 Poitiers Cedex 9, France.*

[2] *Eau de Paris, Direction de la Recherche & Développement et de la Qualité de l'Eau, 33 avenue Jean Jaurès, 94200 Ivry-Sur-Seine, France.*

[3] *Institute of Electron Microscopy and Nanoanalysis, NAWI Graz, Graz University of Technology, Steyrergasse 17, 8010 Graz, Austria.*

** Corresponding author, E-mail: benoit.teychene@univ-poitiers.fr*

Abstract

It is well recognized that chlorine is responsible for aging of membrane materials. The goal of this study is to investigate the modifications of a commercial PES/PVP hollow fiber membrane exposed to hypochlorite solution at pH 7.5 by continuous filtration. Thanks to ATR-FTIR 2D Correlation Spectroscopy (2DCoS) analysis it was confirmed that PVP is oxidized into succinimide compound. 2DCoS analysis revealed the sequence order of PES/PVP membrane degradation: PVP oxidation is followed by the modifications of C-H cyclic structures and finally the formation of succinimide compounds. ATR-FTIR-microscopy mapping unveiled that PVP was mainly situated at the inner surface of hollow fibers exhibiting initially a 67 µm thickness layer. PVP layer disappearance was not homogenous versus the exposure dose suggesting the topochemical character of the PVP-chlorine reaction. Results demonstrate that advanced material characterization are key methodologies to understand membrane aging mechanisms.

Keywords: Ultrafiltration, Membrane aging, Sodium hypochlorite, PES/PVP membrane, 2DCoS, FTIR-Mapping

1. Introduction

Nowadays membrane processes dominate the market of drinking water treatment facilities [1]. In most installations membrane operators manage the impact of membrane fouling through frequent cleaning procedures. Typically in drinking water processes, the cleaning methods include hydraulic flushing by membrane backwash using chlorinated permeate and chemical cleaning by soaking (cleaning in place) with sodium hypochlorite (NaOCl), caustic soda or acidic solutions. Their primary goal is to reduce biofilm growth on the membrane surface as hypochlorite presents high biocidal activity [1].

In past years NaOCl impact on membrane material has raised the attention of researchers due to its high dose (from $mg.L^{-1}$ to several $g.L^{-1}$), frequent use, high exposure time and strong oxidant properties [2–4]. It is commonly reported that chlorine oxidizes the membrane polymers (i.e.: polyethersulfone PES, polysulfone PSU or polyvinylpyrrolidone PVP) and specifically the pore forming additives (i.e: PVP). These reactions might cause membranes' polymer chain scission and formation of new end groups depending on the investigated membrane materials [5–7].

Whatever the membrane materials the main consequence is a change in filtration performance of the membrane such as permeability, fouling resistance, pore size, zeta potential and tensile strength [8,9]. For example Arkhangelsky et al. [6] showed the loss of integrity for PES membranes exposed to chlorine by highlighting chain scissions of the main polymer. In a subsequent study Causserand et al. [10] stated that chlorinated PVP might leak from membrane material and lead to increased permeability and decreased mechanical strength of the membrane. Similarly the aged membranes exhibit a strong tendency to fouling due to changes in membrane hydrophobicity [11–13].

PVP modification under chlorine exposure is often monitored by Attenuated Total Reflectance-Fourier Transform Infrared (ATR-FTIR) analysis at 1650 cm^{-1} (ν C=O). The main oxidization mechanism involves pyrrole ring opening due to chlorine electro addition leading to the formation of by-products such as succinimide compound [3]. Hanafi et al. [14] reported also the formation of succinimide compounds during membrane chlorination. In addition Xie et al. [15] reported a potential formation of chlorinated by-products (i.e.: trihalomethanes (THM)) during membrane exposure to chlorine. Recently Fouquet et al. [16] thanks to MALDI-TOF technique identified the recombination of PVP during hypochlorite oxidation (in homogeneous reaction system) leading to the formation of succinimide. Zhou et al. [13] identified the sequence of a PES/PVP membrane aging under chlorine exposure at three pHs (6, 8 and 10) by using 2D-FTIR correlation spectroscopy (2D-FTIR-CoS): Firstly a change in cyclic C-H structures followed by amide groups modification (i.e.: PVP compounds). Secondly a modification of sulfone ($R\text{-}SO_2\text{-}R$) and aromatic structures at high exposure dose.

In addition the cleaning pH have a strong impact on aging mechanisms due to the different oxidation potential of hypochlorous acid (HOCl) and hypochlorite ion (ClO^-) species (pKa = 7.58 at 20°C). Several articles reported a stronger membrane degradation at pH 8 than at higher pH (usually pH 10-12) [3,14]. Moreover coexistence of HOCl and ClO^- at neutral pH might lead to the formation of hydroxyl radicals ($HO^{\bullet}$) acerbating the polymer chain scission mechanism [17–19].

As this review of the literature points out most studies have reached similar conclusions: chlorine reduces the mechanical resistance of membranes and increases fouling tendency due to the oxidation of PVP within the polymer. However, despite several studies, mechanisms of polymers degradation with chlorine are still ambiguous because of the complexity of heterogeneous reaction system.

The main goal of this study is to investigate the modifications of a commercial PES/PVP hollow fiber membrane exposed to hypochlorite solution at pH 7.5 using realistic exposition conditions (filtration of chlorine solution in dead end mode with similar concentration as used during membrane backwash on site (30 mg Cl_2 L^{-1})). Membranes modifications were analyzed using advanced infrared techniques and data analysis: ATR-FTIR, 2D correlation spectroscopy analysis, FTIR mapping. This study will help to better understand time and chlorine dose dependent mechanisms of the degradation of PES/PVP membranes.

2. Material and methods

2.1 Membrane and lab scale filtration pilot

Commercial PES/PVP hollow fiber membranes were used for this study. According to manufacturer the membrane's pore size is about 20 nm with a corresponding molecular weight cut-off (MWCO) of 150 kDa and the pure water permeability is about 700 ± 30 $L.h^{-1}.bar^{-1}.m^{-2}$. All other characteristics are listed in Table S1. For every experiment a new hollow fiber membrane was potted in a polyamide tube (inner diameter: 4.0 mm) with an epoxy resin (Araldite 2012). One end of every module was left open to allow dead-end inside-out filtration mode. The mini-module consisted of one fiber 25 cm long corresponding to a filtration surface of about 50 ± 6 cm^2. Experiments were performed on a filtration pilot as previously described [20]. The mini-module was inserted in a polytetrafluoroethylene (PTFE) casing with a volume of 27 ± 5 mL. One peristaltic pump (Masterflex®L/S® Cole - Parmer®) was used for dead-end inside-out filtration. The transmembrane pressure and temperature were continuously recorded using Endress + Hauser® sensors (pressure sensor with flush membrane series 8020 and compact temperature sensor, M12 connector, series 2120). Membranes were deconditioned prior to every aging test for a minimum of 24 hours with MilliQ water to remove preservatives and to wet pores. Then the pure water flux of the membrane was measured by the flux step method using permeate flux ranging from 24 to 180

$L.h^{-1}.m^{-2}$ (2 to 15 $mL.min^{-1}$). All permeabilities were corrected at 20°C ($L_{P(20°C)}$ in $L.m^{-2}.h^{-1}.bar^{-1}$) and calculated using the Darcy's law (equation 1).

$$L_{P(20°C)} = \frac{Q_P}{S \times \Delta P_m} \times e^{\left(3{,}056 \times \frac{(20-T)}{(105-T)}\right)} \quad \text{[Eq. 1]}$$

Where ΔP_m, the transmembrane pressure (bar); Q_P, the permeation volumetric flow rate ($L.h^{-1}$); S, the effective surface area of the membrane (m^2) and T, the temperature (°C).

The permeability Lp measured during the chlorine exposure tests were normalized using the initial permeability of the membrane in order to compare results.

Prior and after every filtration test, membrane integrity was verified by a pressure decay test. Membranes were previously moistened in backwash mode with MilliQ water to fill the membrane's casing. Pressurized air was then injected into the fiber lumen at a pressure of 2.0 ± 0.1 bars and the air pressure decay was monitored over at least 10 minutes. The threshold for validation of membrane integrity and the system tightness was fixed at a maximum pressure loss of 200 mbars after 10 minutes [21].

2.2 Chlorine degradation test conditions

The experiments were carried out with sodium hypochlorite (Univar) for chlorine degradation at pH 7.5 for a maximum chlorine exposure of 4500 $mg.h.L^{-1}$ (C×t). A total of six membranes were aged with increasing exposure times (from 4.2 to 150 hours) and a constant concentration of free chlorine (FC) of 30 $mgCl_2.L^{-1}$. Experiments were at least duplicated. Compared with previous studies, the free chlorine concentration was similar to the concentration conventionally used for chemically enhanced backwashing on drinking water production site. In drinking water production plant, chlorine washes are done every 65 minutes (i.e.: 22 times a day) with a free chlorine concentration of 4 $mg.L^{-1}$. Washes last 70 seconds. So the chlorine exposure dose per day is of 1.7 $mg.h.L^{-1}$ and in the experiments the maximum exposure dose of 4500 $mg.h.L^{-1}$ is then equivalent to a period of membranes use of about 7 years in drinking water production plant.

The filtration rate is fixed using a peristaltic pump (Masterflex®L/S® Cole - Parmer®) to obtain a permeate flow of 195 ± 5 $L.h^{-1}.m^{-2}$. pH (SenTix WTW pH probe), flow rate and FC are measured three times a day and adjusted if necessary. FC is determined by the diethyl-p-phenylenediamine (DPD) colorimetric method (USEPA 0330.5) using a Hach® Pocket Colorimeter II ™ and free chlorine concentration kept constant by adding chlorine from a concentrated solution [22]. The transmembrane pressure and the temperature of solution are recorded every minute by Comark® data loggers connected to Endress + Hauser® pressure and temperature sensors. At the end of the chlorine degradation test membranes are backwashed for 24 hours with MilliQ water to remove traces of chlorine prior FTIR analysis.

2.3 Characterizations of membranes materials

2.3.1 Attenuated total reflectance Fourier transform Infrared spectroscopy (ATR-FTIR)

Every membrane fiber was analyzed by ATR-FTIR spectroscopy in order to highlight the characteristic groups of its main constituents. For this, 1 cm of every hollow fiber membrane was split lengthwise with a surgical knife and ATR-FTIR analysis was done on the inner surface of membranes' canals. The analyses were carried out using a NEXUS 6700 Thermo Nicolet Fourier transform infrared spectrometer in a wave number range from 4000 to 600 cm^{-1}. 16 scans were realized with a scan rate of 0.63 $cm.s^{-1}$ and the spectral resolution was of 4 cm^{-1}. The crystal is a diamond and the detector is a Deuterated TriGlycine Sulfate (DTGS). ATR-FTIR spectra are computed using the ChemoSpec (version 4.4.97) package in R-Studio software. Prior to 2D-FTIR Cos analysis all spectra were baseline corrected (using a polymer fit model), normalized using probabilistic quotient normalization method provided by the ChemoSpec package version 4.4.97.

2.3.2 2D Correlation spectroscopy analysis

Two-dimensional correlation spectroscopy is used in order to find out significant variations in spectral intensities [13]. The external perturbation applied to the system is the exposure dose (Ct) used in dynamic membrane aging. This method has been increasingly used to determine correlations between spectral and sequential changes of functional groups induced under a perturbation (for example the chlorine exposure dose). In reference to Noda studies, dynamic spectrum $\tilde{A}(\nu, Ct)$ (equation 2), Synchronous $\Phi(\nu_1,\nu_2)$ and Asynchronous $\Psi(\nu_1,\nu_2)$ spectra were defined. Calculation details of synchronous $\Phi(\nu_1,\nu_2)$ and asynchronous $\Psi(\nu_1,\nu_2)$ spectra are given in Supplementary data [23,24]. The value of $\Phi(\nu_1,\nu_2)$ represents the coincidental changes observed at wavenumber ν_1 and ν_2 during the interval of the chlorine exposure (Ct_{min} and Ct_{max}). In contrast, the value of $\Psi(\nu_1,\nu_2)$ in asynchronous spectra can inform on the

sequential order changes of wavenumber ν_1 and ν_2 during the variation of the considered perturbation variable (i.e.: exposure dose).

$$\tilde{A}(\nu, Ct) = \{A(\nu, Ct) - \bar{A}(\nu)\} \text{ for } Ct_{min}<Ct<Ct_{max} \text{ ; 0 if not} \quad \text{[Eq. 2]}$$

Where the reference spectrum $\tilde{A}(\nu)$ is the averaged spectrum between the minimum and the maximum chlorine exposure (Ct_{min} and Ct_{max} namely, 0 and 4500 $mg.h.L^{-1}$, respectively) ν, the wavenumber in ATR-FTIR spectra.

$\bar{A}(\nu)$ is defined by the equation 3.

$$\bar{A}(\nu) = \frac{1}{m}\sum_{i=1}^{m} A(\nu, Ct) \quad \text{[Eq. 3]}$$

Where m, the number of spectra.

The FTIR 2D correlation spectroscopy analysis was performed using R-Studio software using the corr2D package version 0.2.0 [25].

2.3.3 FTIR mapping

The analysis is carried out by a Hyperion 3000 FTIR microscope coupled to a Tensor27 spectrometer (Bruker, Billerica, USA). The samples are prepared according to previous published work [26]. Hollow fiber is glued in epoxy resin (EpoHeat® with a low FTIR response) and then cut into thin slices of 20 µm. FTIR analyses are respectively targeted at the wavenumbers of 1570 cm^{-1} (C = C ring bond of PES) and 1650 cm^{-1} (C = O bond of PVP) in order to investigate membrane materials changes at several chlorine dose exposures.

2.3.4 Thermal analyzes (DTA/TGA/DSC)

After aging, the degradation temperature of the materials and the heat flux associated with the phase transitions were determined. Membrane samples were analyzed by DTA/TGA/DSC in order to evaluate the thermal properties of the aged polymer blend in aged membranes. These

analysis were performed using an SDT Q600 (TA Instrument). For that, membrane samples (mass ranged from 4 to 15 mg) were placed inside a crucible for calcination in air at 800 °C at a rate of 10 °C per minute.

3. Results and discussion

3.1 Membrane aging – simulation by chlorine exposure

Figure 1 shows the evolution of the relative permeability L_P/L_{P0} for different chlorine exposures. In absence of chlorine the filtration of MilliQ water at pH 7.5 for 150 hours showed a constant permeability of 699 ± 31 $L.h^{-1}.m^{-2}.bar^{-1}$. Samples were denominated according to their maximum exposition dose (i.e: Ct 4500 corresponds to a fiber exposed to 30 mg L^{-1} for 150 hours). The permeability variation was provided in supplementary data (Fig S1.)

Furthermore results obtained for 6 different samples of membranes exhibit the increase of permeability with increasing chlorine exposures from 125 to 4500 mg.h.L-1 (i.e. for reaction times from 4 to 150 hours and a 30 $mgCl_2.L^{-1}$ chlorine solution). Similar profiles were obtained for all investigated fibers. The permeability at 4500 $mgCl_2.h.L^{-1}$ was 2.5 times higher than the initial permeability (1721 ± 30 versus 727 ± 32 $L.h^{-1}.m^{-2}.bar^{-1}$ for the aged and pristine membranes, respectively).

The relative permeability evolution shaped a sigmoid curve during aging process (Insert in Figure 1). Indeed the initial permeability was stable for the first 2.5 hours of filtration, which can be linked to a phase of initiation of the solid-liquid reaction between NaOCl and polymer. Then, a rapid increase in permeability was observed between 2.5 and 33 h (i.e. 75 and 1000 $mg.h.L^{-1}$) to achieve a permeability of 1434 ± 15 $L.h^{-1}.m^{-2}.bar^{-1}$ (1.8 times the initial permeability). From 1000 $mg.h.L^{-1}$ the increase of the permeability slowed down and tended towards an asymptote. According to the pressure decay test, no loss of integrity was observed

for all fibers studied and exposure doses. The increase of permeability is generally related to the oxidation of membrane polymers and in particular PVP with hypochlorous acid (HOCl) [27]. These results are consistent with previous studies of Abdullah and Bérubé [28] and Causserand et al. [10] showing a strong increase in permeability for low chlorine exposures and slight variation at high exposure.

3.2 IR characterization of membrane materials

3.2.1 Characterization by conventional ATR-FTIR analysis

Figure S2 represents a survey of all IR spectra of PVP-PES membrane at different chlorine exposures. The main variations of the IR spectra are the decrease of the peak intensity at 1650 cm^{-1}. In addition, one can observe, the appearance of peak at 1700 and 1770 cm^{-1} at high exposure doses (Fig. S2). The peak at 1650 cm^{-1} is relative to the stretching of C=O bond in PVP. Peak at 1700 and 1770 cm^{-1} are characteristic of asymmetric and symmetric stretching of the imide function in succinimide, respectively [3,29]. While the decrease in PVP peak begin with chlorine exposure of 125 $mg.h.L^{-1}$, succinimide peak appears at the highest chlorine exposure of 4500 $mg.h.L^{-1}$. These modifications attest to the oxidation of PVP by chlorine [30]. Other peak variations, with a lower extent, might be observed at 1105, 1150, 1290, 1240, 1400-1460 cm^{-1} corresponding to the symmetric & asymmetric vibration of the sulfone groups of PES (υ_{as} R-SO_2-R), aromatic ether structure (R-O-R) and the cyclic C-H structures of pyrrolidine of PVP, respectively.

Figure 2 shows the evolution of normalized permeability compared to normalized absorbance at 1650 cm^{-1} determined after the 6 different chlorine exposures (obtained on 6 different membranes). Results showed that the increase in permeability was correlated linearly (Pearson Coefficient R =-0.933 & p-value = 0.0066, n = 7) with the decrease of the IR absorbance at 1650 cm^{-1}. The increase in permeability can be attributed to the loss of PVP

within the membrane which would increase the pore size [6]. However, more experimental data are needed to fully demonstrate the linear relation.

3.2.2 2D Correlation spectroscopy analysis (2DCoS)

In order to further investigate polymers change during aging process and to elucidate modification sequence, 2D correlation spectra are plotted (Homo correlation, Figure 3). Both spectra are focused on the region between 1000 and 1800 cm^{-1} where the main variations are observed. Synchronous and asynchronous correlation spectra are reported in Figure 3a & 3b, respectively.

Eight auto-peaks centered at 1105, 1146, 1240, 1290, 1480, 1580, 1650, 1700 cm^{-1} could be identified in the synchronous spectrum (Figure 3a). The highest intensities are observed for 1105, 1150, 1240, 1650 cm^{-1} wavenumber. The succinimide group auto-peak at 1700 cm^{-1} has a low intensity indicating a slight change during membrane chlorination (Figure 3a). The auto-peaks related to the cyclic C-H structures of pyrrolidine of PVP at 1410, 1446 and 1460 cm^{-1} have also low intensity indicating slight change during chlorine exposure. As observed by Zhou et al. [13], no auto-peak is observed at 1030 cm^{-1} attributed to sulfonic acids or phenolic groups. This might be due to the low amount of PVP present in the commercial hollow fiber membranes (lower than 5%) and the low chlorine exposures used during aging process. Indeed DTA/TGA/DSC thermal analyzes of the new and chlorine-aged membrane samples at pH 7.5 Ct 2700 and Ct 4500 $mg.h.L^{-1}$ are performed (Figure S3). The peak at 450°C on differential thermogravimetric (DT) curve corresponds to the thermal degradation of PVP [31]. At this temperature, thermal analysis shows a mass loss of about 3% for the new membrane, attributable to the amount of PVP in the membrane. In addition, the higher the Ct the more the peak decreases at this temperature (Figure S3-a&b). This variation confirms the deterioration of PVP during aging.

For sake of simplicity, the cross-peaks interpretation is only done with respect to the signal variation at 1650 cm^{-1}, corresponding to the C = O vibration of amide groups of PVP ($\Phi(\nu_1,1650)$ and depicted by the horizontal dashed line in Figure 3 a & b. Positive correlations ($\Phi(\nu_1, 1650) > 0$, red color) are observed for wavenumbers of 1290, 1440, 1460 cm^{-1} indicating that spectral intensities at these wavenumbers slightly decrease with respect to the exposure dose.

Other synchronous correlations with 1650 cm^{-1} including those at 1105, 1146, 1240 and 1480 cm^{-1} have a negative sign indicating that the aromatic and sulfone groups increase in intensity under the investigated hypochlorite exposure dose range. However due to the low correlation value obtained ($R < -3.1\ 10^{-4}$) this observation might be attributed to the FTIR absorbance variation due to polymer sample variation (analysis performed on seven different membranes).

The synchronous spectrum shows that the succinimide peak (1700 cm^{-1}) increases when the PVP signal decreases demonstrating the formation of succinimide associated to PVP oxidation [7,13]. In asynchronous spectrum, one can see that the signal intensity of succinimide appeared after the decrease of PVP signal ($\Phi(1700, 1650) < 0$ & $\Psi(1700, 1650)>0$). Also figure 3, suggests that succinimide formation is the final observed step regarding PVP oxidation according to the maximum investigated exposure dose ($\Phi(\upsilon_1, 1700) < 0$ & $\Psi(\upsilon_1, 1700)<0$).

Presented results demonstrate that membranes aging occurs in a specific sequence. In the asynchronous spectrum, negative correlations observed between (1446 and 1460 cm^{-1}) and 1650 cm^{-1} indicates that C = O bond of PVP decreases before a decrease in the bands associated with cyclic structures. Negative correlations are also observed between 1650 cm^{-1} and 1700 cm^{-1} suggesting that the PVP signal decreases in intensity before the formation of succinimide. It can also be concluded that the reduction of cyclic structures occurs before the

formation of succinimide as evidenced by negative correlations between 1446, 1460 and 1700 cm^{-1}. Intensity order changes associated to sulfone and aromatic groups could not be determined since these correlations exhibited split contours. This sequence is consistent with previous reported results [13, 7]. However lower correlations are obtained in the present study probably due to lower investigated exposure dose and the different hollow fiber used compared to Zhou et al. (maximum 216,000 $mg.h.L^{-1}$) [13]. Reported results emphasize that at low exposition dose (lower than 4500 mg h L^{-1}) only the PVP is oxidized by chlorine and slight or negligible changes are observed for the PES material. This last point is confirmed by ATR-FTIR microscopy mapping (see section 3.2.3).

In contrast to raw ATR-FTIR spectra comparison usually performed, 2D correlation spectroscopy is a powerful methodology to analyze hollow fiber membrane degradation during chemical aging.

3.2.3 Characterization by ATR- FTIR-microscopy mapping

The maps obtained by ATR-FTIR analysis coupled to microscopy are presented in Figure 4 for a new membrane rinsed with MilliQ water (Ct 0, Fig.4, images a & h) and the 6 membranes aged at pH 7.5.The upper images (Figures 4a to 4g) presents mapping of PES signal obtained at 1570 cm^{-1} and lower images (Figure 4h to 4n) mapping of PVP signal at 1650 cm^{-1}. SEM pictures provided in supplementary data for a new rinsed membrane and the membrane exposed at 4500 mg h L^{-1} failed to identify coarse structural changes in membrane material (FigS4).

As shown in Figure 4 the light blue color represents the hollow fiber lumen with a radius of 0.45 mm approximately (Image scale: 0.4 mm ≡ 1.6 cm). The PES signal in Figures 4a to 4g is rather homogeneous. Exposure to chlorine does not have a visible impact on PES mapping in the studied aging conditions investigated (Ct_{max} = 4500 $mg.h.L^{-1}$). It is important to note that the image contrast of Figure 4g was accentuated in order to distinguish PVP signal in

Figure 4n. The absence of major modifications in PES (1570 cm^{-1}) at maximum investigated exposure dose is consistent with bibliographic data obtained for similar conditions [26,32].

The image in Figure 4h obtained at Ct = 0 makes it possible to visualize the skin located at the inner surface of the filtration channels of the hollow fiber membrane with a strong presence of PVP (FTIR wavenumber at 1650 cm^{-1}, Fig. 4h). Interestingly PVP is only located at the inner surface which is due to the manufacturing process and the high molecular weight of PVP [33]. The thickness of the PVP layer is estimated at 65 μm.

FTIR maps reported in Fig.4 h-n highlight the decrease of PVP signal with increasing Ct. For Ct < 500 $mg.h.L^{-1}$ PVP shows a uniform layer but intensity of PVP signal decreases with increasing exposure dosed. Only scattered PVP spots remain visible for higher exposure doses ranged from 500 to 2700 $mg.h.L^{-1}$. At 4500 $mg.h.L^{-1}$ the PVP signature cannot be analyzed even though the image contrast was accentuated. The FTIR mapping is in accordance with the three phases observed in Figure 1 during membrane aging. The PVP layer and permeability remains similar to the native membrane for Ct < 75 $mg.h.L^{-1}$. From 75 to 1000 $mg.h.L^{-1}$ the permeability strongly increases and the signal of the PVP layer decreases quickly. Finally, for the highest investigated exposure doses (1000 to 4500 $mg.h.L^{-1}$), permeability and intensity of the PVP spots variation slow down.

These results show that the PVP reaction with chlorine was not homogenous suggesting the “topochemical” character of the solid-liquid reactions occurring during chemical membranes aging [34]. Indeed reported results suggest that some PVP regions within the membrane polymer are less accessible to chlorine and consequently react slowly or are governed by chlorine diffusion.

To conclude FTIR mapping appears as a powerful tool for studying membrane aging because it reveals how the membrane materials is modified by chlorine. The results demonstrate more

specifically that the membrane aging might be considered as a non-steady-state topochemical process [35].

4. Conclusion

This study confirms the complexity of PES/PVP hollow fibers membrane aging under hypochlorite exposure. Thanks to the specific aging protocol used consisting in a continuous filtration of hypochlorite solution at pH 7.5 (30 $mgCl_2.L^{-1}$) it was possible to deeply investigate PVP changes. First, the permeability monitoring during aging showed an increase in two stages. ATR-FTIR classical analysis observed at 1650 cm^{-1} has been linearly correlated to changes in permeability.

Advanced data analyses of FTIR spectra and FTIR mapping have been employed in order to intensify membrane diagnosis. Main conclusions are:

- 2DCoS analysis unveiled the sequence order of PES/PVP membrane degradation as follow: decrease of amide groups (PVP band) then modification of the C-H cyclic structures changing and finally the formation of succinimide compound. Peak related to aromatic and sulfone groups showed split contour making order assignment difficult to assess at this low chlorine exposure dose.
- ATR-FTIR-microscopy mapping demonstrated that PVP oxidation is not homogenous and some regions are less accessible to chlorine oxidation. This observation suggests that hollow fibers chemical aging is a non-steady-state topo-chemical process.

Finally, this study shows the interest of diagnostic tools such as ATR-FTIR 2D Correlation spectroscopy analysis and microscopy coupled with infrared detection to follow and characterize the aging state of the membrane material. Moreover such methodologies might be useful to develop membrane chemical aging model by taking into account the specific kinetic regime in the membrane.

Acknowledgement

The authors thank Manfred Nachtnebel from Institute of Electron Microscopy and Nanoanalysis (Graz, Austria) for spatial characterization analyses.

References

[1] X. Shi, G. Tal, N.P. Hankins, V. Gitis, Fouling and cleaning of ultrafiltration membranes: A review, J. Water Process Eng. 1 (2014) 121–138. doi:10.1016/j.jwpe.2014.04.003.

[2] K. Yadav, K.R. Morison, Effects of hypochlorite exposure on flux through polyethersulphone ultrafiltration membranes, Food Bioprod. Process. 88 (2010) 419–424. doi:10.1016/j.fbp.2010.09.005.

[3] R. Prulho, S. Therias, A. Rivaton, J.-L. Gardette, Ageing of polyethersulfone/polyvinylpyrrolidone blends in contact with bleach water, Polym. Degrad. Stab. 98 (2013) 1164–1172. doi:10.1016/j.polymdegradstab.2013.03.011.

[4] C. Regula, E. Carretier, Y. Wyart, G. Gésan-Guiziou, A. Vincent, D. Boudot, P. Moulin, Chemical cleaning/disinfection and ageing of organic UF membranes: A review, Water Res. 56 (2014) 325–365. doi:10.1016/j.watres.2014.02.050.

[5] V. Gitis, R. Haught, R. Clark, J. Gun, O. Lev, Application of nanoscale probes for the evaluation of the integrity of ultrafiltration membranes, J. Membr. Sci. 276 (2006) 185–192. doi:10.1016/j.memsci.2005.09.055.

[6] E. Arkhangelsky, D. Kuzmenko, V. Gitis, Impact of chemical cleaning on properties and functioning of polyethersulfone membranes, J. Membr. Sci. 305 (2007) 176–184. doi:10.1016/j.memsci.2007.08.007.

[7] Y. Kourde-Hanafi, P. Loulergue, A. Szymczyk, B. Van der Bruggen, M. Nachtnebel, M. Rabiller-Baudry, J.-L. Audic, P. Pölt, K. Baddari, Influence of PVP content on degradation of PES/PVP membranes: Insights from characterization of membranes with controlled composition, J. Membr. Sci. 533 (2017) 261–269.

[8] S. Robinson, S.Z. Abdullah, P. Bérubé, P. Le-Clech, Ageing of membranes for water treatment: Linking changes to performance, J. Membr. Sci. 503 (2016) 177–187. doi:10.1016/j.memsci.2015.12.033.

[9] Y. Zhang, J. Wang, F. Gao, Y. Chen, H. Zhang, A comparison study: The different impacts of sodium hypochlorite on PVDF and PSF ultrafiltration (UF) membranes, Water Res. 109 (2017) 227–236. doi:10.1016/j.watres.2016.11.022.

[10] C. Causserand, B. Pellegrin, J.-C. Rouch, Effects of sodium hypochlorite exposure mode on PES/PVP ultrafiltration membrane degradation, Water Res. 85 (2015) 316–326. doi:10.1016/j.watres.2015.08.028.

[11] H.D.W. Roesink, M.A.M. Beerlage, W. Potman, T. van den Boomgaard, M.H.V. Mulder, C.A. Smolders, Characterization of new membrane materials by means of fouling experiments Adsorption of bsa on polyetherimide—polyvinylpyrrolidone membranes, Colloids Surf. 55 (1991) 231–243. doi:10.1016/0166-6622(91)80095-6.

[12] A. Touffet, J. Baron, B. Welte, M. Joyeux, B. Teychene, H. Gallard, Impact of pretreatment conditions and chemical ageing on ultrafiltration membrane performances. Diagnostic of a coagulation/adsorption/filtration process, J. Membr. Sci. 489 (2015) 284–291. doi:10.1016/j.memsci.2015.04.043.

[13] Z. Zhou, G. Huang, Y. Xiong, M. Zhou, S. Zhang, C.Y. Tang, F. Meng, Unveiling the Susceptibility of Functional Groups of Poly(ether sulfone)/Polyvinylpyrrolidone Membranes to NaOCl: A Two-Dimensional Correlation Spectroscopic Study, Environ. Sci. Technol. 51 (2017) 14342–14351. doi:10.1021/acs.est.7b03952.

[14] Y. Hanafi, P. Loulergue, S. Ababou-Girard, C. Meriadec, M. Rabiller-Baudry, K. Baddari, A. Szymczyk, Electrokinetic analysis of PES/PVP membranes aged by sodium hypochlorite solutions at different pH, J. Membr. Sci. 501 (2016) 24–32. doi:10.1016/j.memsci.2015.11.041.

[15] P. Xie, C.-F. de Lannoy, J. Ma, M.R. Wiesner, Chlorination of polyvinyl pyrrolidone–polysulfone membranes: Organic compound release, byproduct formation, and changes in membrane properties, J. Membr. Sci. 489 (2015) 28–35. doi:10.1016/j.memsci.2015.03.058.

[16] T. Fouquet, M. Torimura, H. Sato, Multi-stage Mass Spectrometry of Poly(vinyl pyrrolidone) and Its Vinyl Succinimide Copolymer Formed upon Exposure to Sodium Hypochlorite, Mass Spectrom. 5 (2016) A0050. doi:10.5702/massspectrometry.A0050.

[17] I.M. Wienk, E.E.B. Meuleman, Z. Borneman, T. van den Boomgaard, C.A. Smolders, Chemical treatment of membranes of a polymer blend: Mechanism of the reaction of hypochlorite with poly(vinyl pyrrolidone), J. Polym. Sci. Part Polym. Chem. 33 (1995) 49–54. doi:10.1002/pola.1995.080330105.

[18] C. Causserand, S. Rouaix, J.-P. Lafaille, P. Aimar, Degradation of polysulfone membranes due to contact with bleaching solution, Euromembrane 2006. 199 (2006) 70–72. doi:10.1016/j.desal.2006.03.144.

[19] C. Causserand, S. Rouaix, J.-P. Lafaille, P. Aimar, Ageing of polysulfone membranes in contact with bleach solution: Role of radical oxidation and of some dissolved metal ions, Chem. Eng. Process. Process Intensif. 47 (2008) 48–56. doi:10.1016/j.cep.2007.08.013.

[20] B. Teychene, A. Touffet, J. Baron, B. Welte, M. Joyeux, H. Gallard, Predicting of ultrafiltration performances by advanced data analysis, Water Res. 129 (2018) 365–374. doi:10.1016/j.watres.2017.11.023.

[21] USEPA, D6908-06(2017), Standard Practice for Integrity Testing of Water Filtration Membrane Systems, ASTM International, United States, (n.d.). www.astm.org.

[22] USEPA, Methods for Chemical Analysis of Water and Wastes. Revised March 1983. EPA 600/4-79-020. Method 0330.5. Chlorine, Total Residual - Spectrophotometric, United States, (n.d.).

[23] Y. Park, I. Noda, Y.M. Jung, Two-dimensional correlation spectroscopy in polymer study, Front. Chem. 3 (2015) 14. doi:10.3389/fchem.2015.00014.

[24] I. Noda, Two-dimensional correlation analysis of spectra collected without knowing sampling order, J. Mol. Struct. 1156 (2018) 418–423. doi:10.1016/j.molstruc.2017.11.085.

[25] R. Geitner, R. Fritzsch, T. Bocklitz, J. Popp, J. Package Version 0.2.0 Implementation of 2D Correlation Analysis in R, (n.d.). https://cran.r-project.org/web/packages/corr2D/corr2D.pdf.

[26] M. Nachtnebel, H. Fitzek, C. Mayrhofer, B. Chernev, P. Pölt, Spatial localization of membrane degradation by in situ wetting and drying of membranes in the scanning electron microscope, J. Membr. Sci. 503 (2016) 81–89. doi:10.1016/j.memsci.2015.12.046.

[27] Y. Hanafi, A. Szymczyk, M. Rabiller-Baudry, K. Baddari, Degradation of Poly(Ether Sulfone)/Polyvinylpyrrolidone Membranes by Sodium Hypochlorite: Insight from Advanced Electrokinetic Characterizations, Environ. Sci. Technol. 48 (2014) 13419–13426. doi:10.1021/es5027882.

[28] S.Z. Abdullah, P.R. Bérubé, Assessing the effects of sodium hypochlorite exposure on the characteristics of PVDF based membranes, Water Res. 47 (2013) 5392–5399. doi:10.1016/j.watres.2013.06.018.

[29] S.M. Louie, J.M. Gorham, J. Tan, V.A. Hackley, Ultraviolet photo-oxidation of polyvinylpyrrolidone (PVP) coatings on gold nanoparticles, Env. Sci Nano. 4 (2017) 1866–1875. doi:10.1039/C7EN00411G.

[30] F. Hassouna, S. Therias, G. Mailhot, J.-L. Gardette, Photooxidation of poly(N-vinylpyrrolidone) (PVP) in the solid state and in aqueous solution, Polym. Degrad. Stab. 94 (2009) 2257–2266. doi:10.1016/j.polymdegradstab.2009.08.007.

[31] V.M. Bogatyrev, N.V. Borisenko, V.A. Pokrovskii, Thermal Degradation of Polyvinylpyrrolidone on the Surface of Pyrogenic Silica, Russ. J. Appl. Chem. 74 (2001) 839–844. doi:10.1023/A:1012717723082.

[32] H. Susanto, M. Ulbricht, Polymeric Membranes for Molecular Separations, in: Membr. Oper., Wiley-Blackwell, 2009: pp. 19–43. doi:10.1002/9783527626779.ch2.

[33] B. Vatsha, J.C. Ngila, R.M. Moutloali, Preparation of antifouling polyvinylpyrrolidone (PVP 40K) modified polyethersulfone (PES) ultrafiltration (UF) membrane for water purification, Phys. Chem. Earth Parts ABC. 67–69 (2014) 125–131. doi:10.1016/j.pce.2013.09.021.

[34] V.V. Boldyrev, Topochemistry and topochemical reactions, React. Solids. 8 (1990) 231–246. doi:10.1016/0168-7336(90)80023-D.

[35] S. Stoeva, L. Vlaev, Kinetics of the Solid-State Chlorination of High-Density Polyethylene, Macromol. Chem. Phys. 203 (2002) 346–353. doi:10.1002/1521-3935(20020101)203:2<346::AID-MACP346>3.0.CO;2-7.

Figure 1: Evolution of relative permeability during aging at pH 7.5 (30mgCl_2.L^{-1}). ○ Membrane 0 – Filtration of MilliQ water at pH 7.5 (Ct 0), ✱Membrane 1 (Ct 125), ◇ Membrane 2 (Ct 250), △Membrane 3 (Ct 500), □Membrane 4 (Ct 1000), ×Membrane 5 (Ct 2700), +Membrane 6 (Ct 4500). *Insert:* Focus on the low exposure dose from 0 to 600 mg h L^{-1} (Membranes 1 to 4)

Figure 2: Relative IR absorbance of C=O bond of PVP (νC=O=1650 cm^{-1}) versus normalized permeability. The relative IR absorbance was calculated as the ratio between IR absorbance of aged membrane A_{PVP} and the IR absorbance of the pristine membrane A_{PVP0}). ○Membrane 0 (Ct 0), ✱Membrane 1 (Ct 125), ◇Membrane 2 (Ct 250), △Membrane 3 (Ct 500), □Membrane 4 (Ct 1000), ×Membrane 5 (Ct 2700), +Membrane 6 (Ct 4500).

Figure 3: Synchronous (a) and asynchronous (b) 2D correlation spectra from ATR-FTIR spectra of aged hollow fibers in PES/PVP. x-axis and y-axis correspond to ν_1 and ν_2, respectively.

Figure 4: FTIR-microscopy mapping done on the cross section of aged hollow fibers as a function of the hypochlorite exposure dose. Images a-g: PES signal obtained at 1570 cm^{-1}; Images h- n: PVP signal obtained at 1650 cm^{-1}.

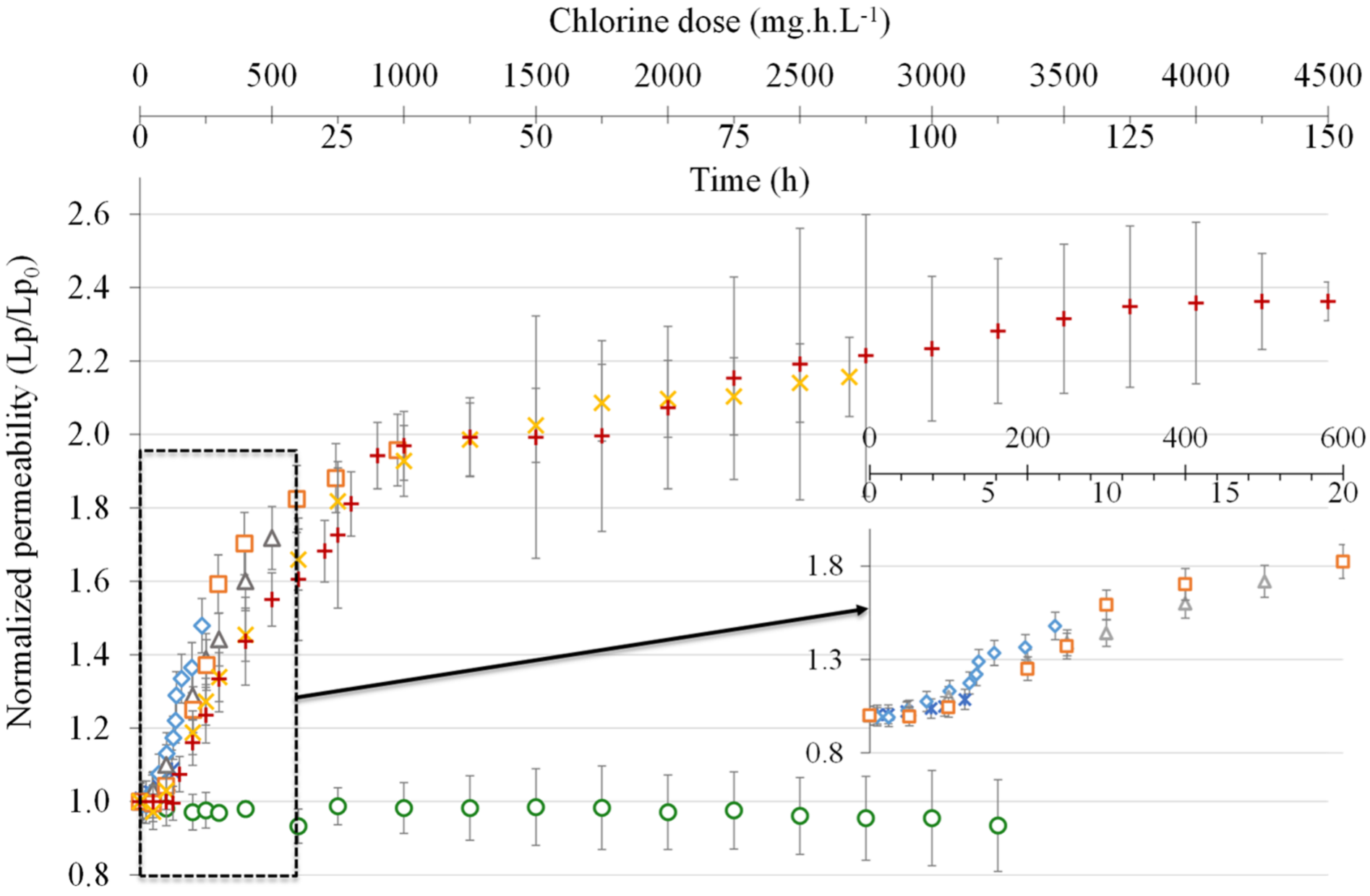
Chlorine dose (mg.h.L-1)
0
500
1000
1500
2000
2500
3000
3500
4000
4500
Time (h)
0
25
50
75
100
125
150
Normalized permeability (Lp/Lp0)
2.6
2.4
2.2
2.0
1.8
1.6
1.4
1.2
1.0
0.8
0
200
400
600
0
5
10
15
20
1.8
1.3
0.8

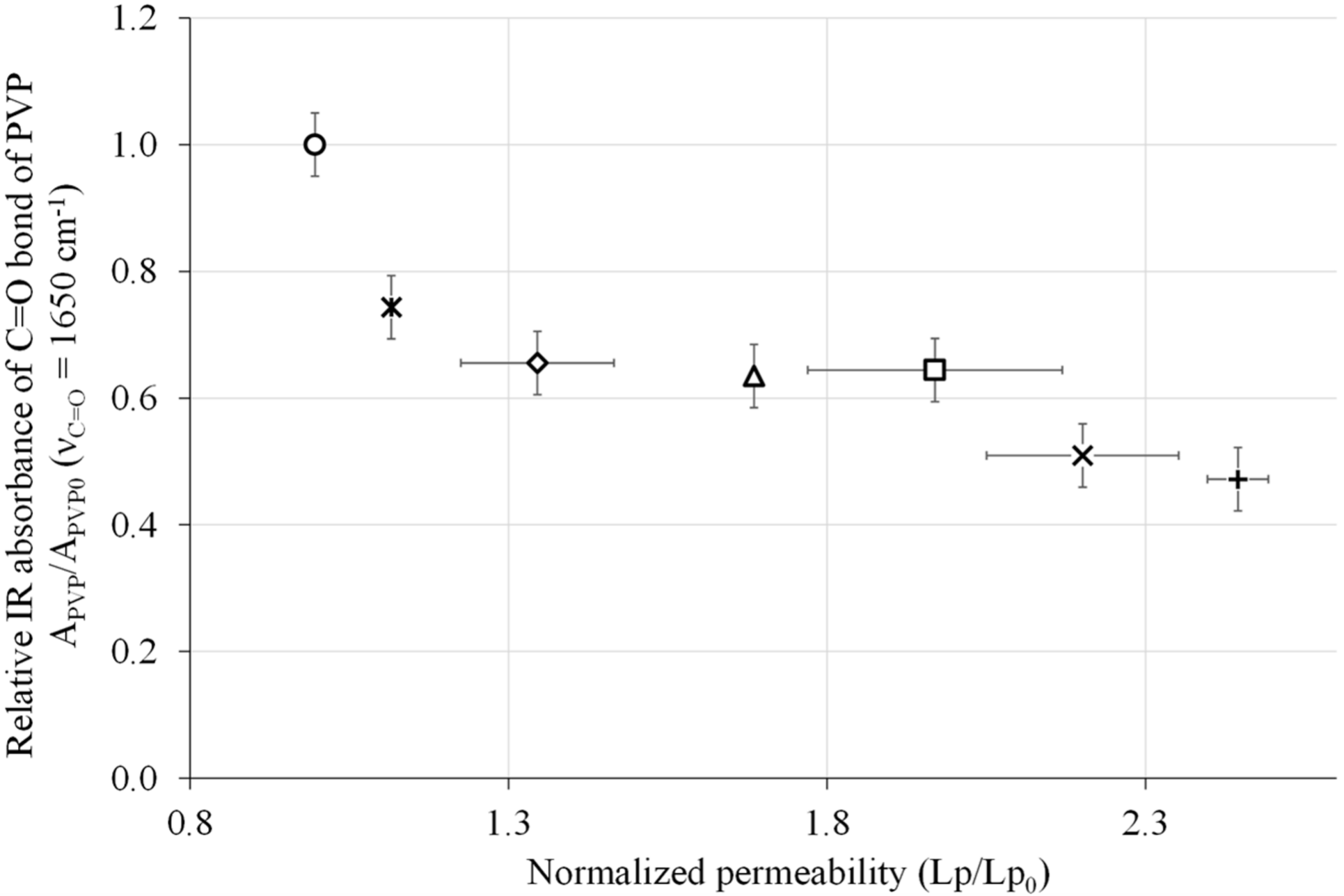
Relative IR absorbance of C=O bond of PVP
A_{PVP}/A_{PVP0} ($\nu_{C=O}$ = 1650 cm^{-1})
1.2
1.0
0.8
0.6
0.4
0.2
0.0
0.8
1.3
1.8
2.3
Normalized permeability (Lp/Lp$_0$)

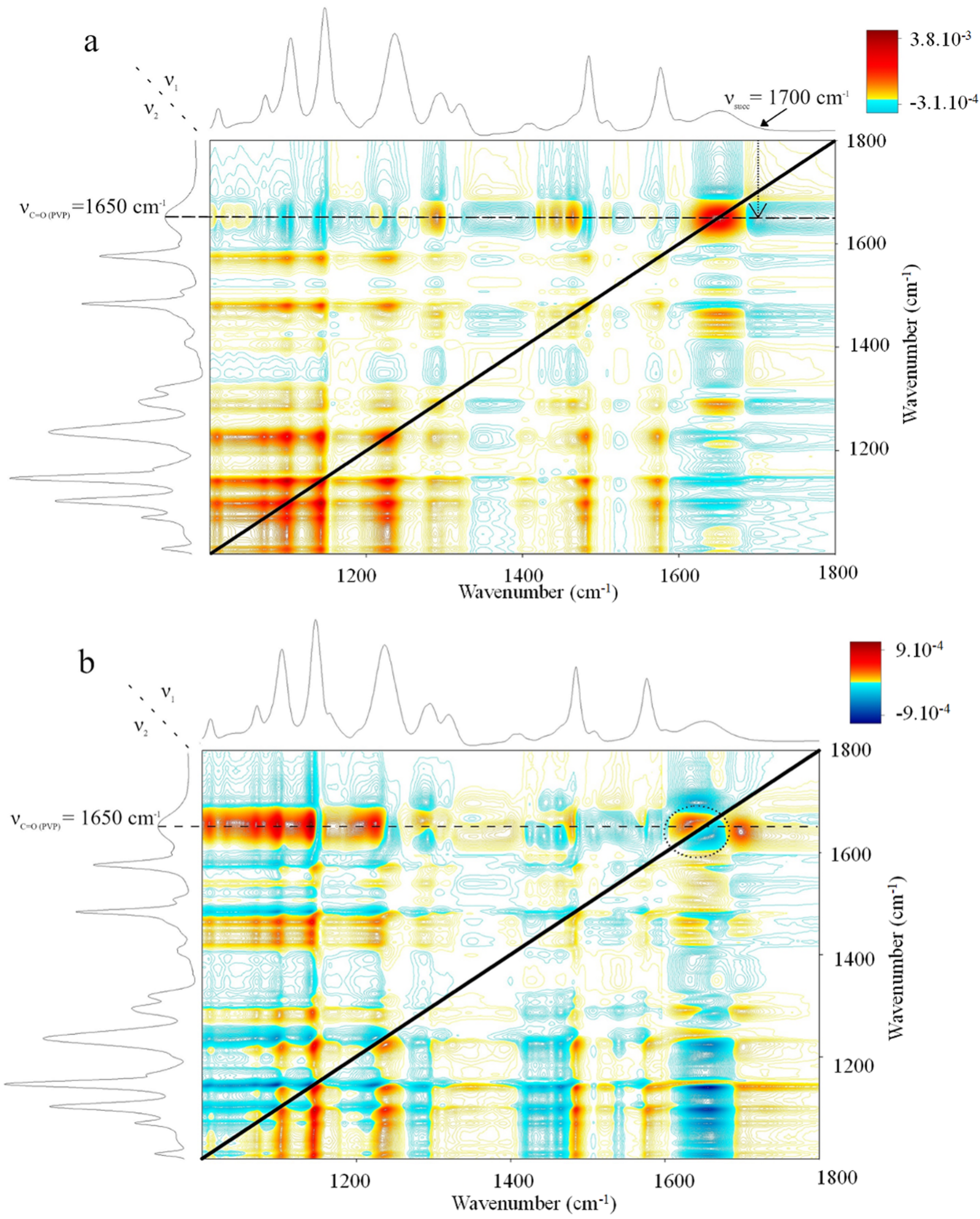
a
ν_1
ν_2
ν_{succ} = 1700 cm^{-1}
3.8.10^{-3}
-3.1.10^{-4}
$\nu_{C=O\ (PVP)}$=1650 cm^{-1}
1800
1600
1400
1200
Wavenumber (cm^{-1})
1200
1400
1600
1800
Wavenumber (cm^{-1})
b
ν_1
ν_2
9.10^{-4}
-9.10^{-4}
$\nu_{C=O\ (PVP)}$ = 1650 cm^{-1}
1800
1600
1400
1200
Wavenumber (cm^{-1})
1200
1400
1600
1800
Wavenumber (cm^{-1})

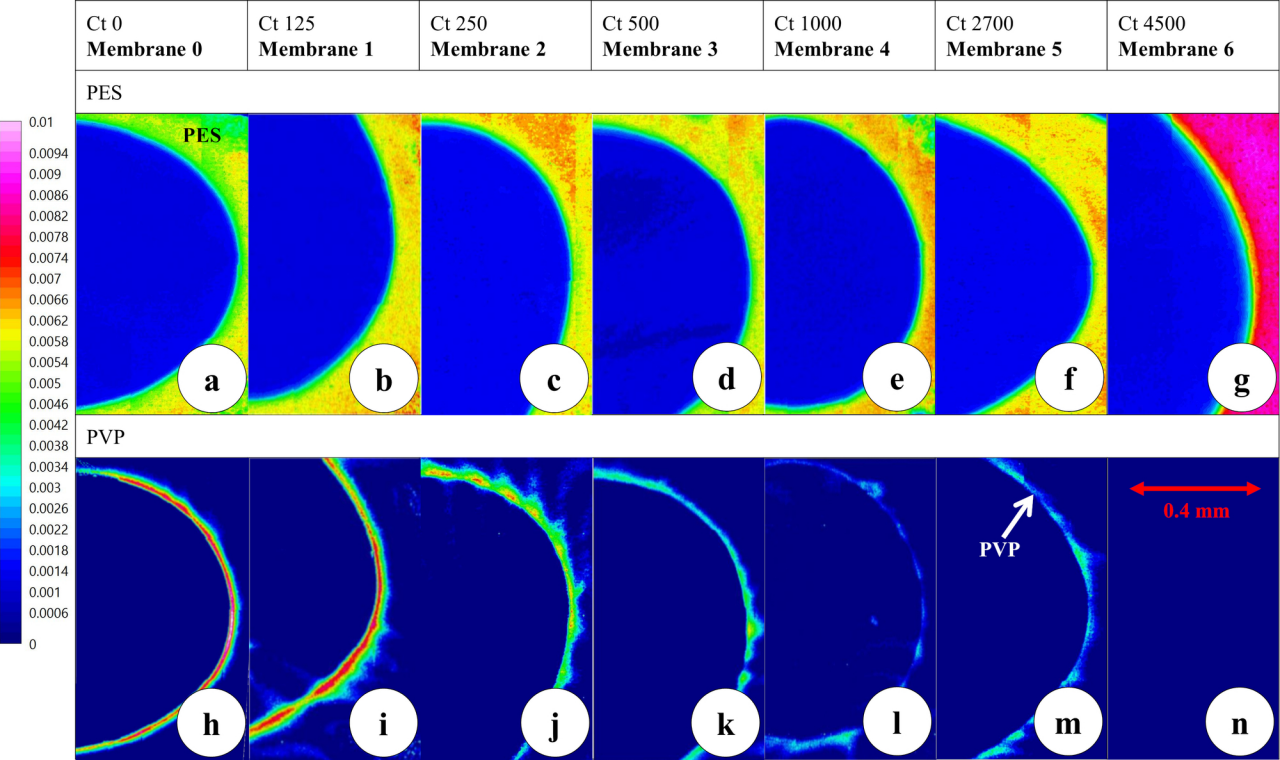
Ct 0
Membrane 0
Ct 125
Membrane 1
Ct 250
Membrane 2
Ct 500
Membrane 3
Ct 1000
Membrane 4
Ct 2700
Membrane 5
Ct 4500
Membrane 6
PES
PES
PVP
PVP
0.4 mm
a
b
c
d
e
f
g
h
i
j
k
l
m
n
0.01
0.0094
0.009
0.0086
0.0082
0.0078
0.0074
0.007
0.0066
0.0062
0.0058
0.0054
0.005
0.0046
0.0042
0.0038
0.0034
0.003
0.0026
0.0022
0.0018
0.0014
0.001
0.0006
0